NCCPM
National Co-ordinating Centre for the Physics of Mammography

Technical evaluation of TiCEM contrast enhanced mammography on the Siemens Revelation system

Technical Report 2201

October 2022

John Loveland, Alistair Mackenzie

Acknowledgements

The authors are grateful to the staff at Royal Stoke University Hospital, Stoke, for their assistance with the evaluation of this equipment.

Funding

This study was funded for the NHS Breast Screening Programme by NHS England and Innovation.

Contents

1. Introduction

1.1 Evaluation report

At the time of publication of this report, the use of contrast enhanced mammography (CEM) is not approved for use in the NHS Breast Screening Programme (NHSBSP). Currently, the technology is being evaluated clinically.

This report is one of a series evaluating the use of CEM on commercially available mammography systems and comprises a summary of the performance of CEM. There is currently no NHSBSP guidance on quality control testing of CEM systems. The methodology developed for this evaluation was primarily derived from two publications by Oduko et al.[1,2]

1.2 Objectives

The purpose of the evaluation was to assess the performance of the TiCEM option for the Siemens Revelation mammography system. The Siemens Revelation full field digital mammography system has previously been evaluated.[3]

1.3 Contrast enhanced mammography description

CEM involves the administration of an iodinated contrast agent followed by the acquisition of two images in close succession; the first at a low energy and the second at a higher energy. These exposures are designed such that the majority of the X-ray spectra is just below the K-edge of iodine in the low energy exposure and just above the K-edge in the higher energy exposure. An algorithm is then applied to create an image without breast structure that shows the location of any iodine accumulation. Such accumulation is a potential indicator of cancer.

2. Methods

The following describes the method for testing the CEM functions. Any system specific testing methods will be described in the results.

2.1 System tested

The system tested is described in Table 1.

Table 1. System description

Location	Royal Stoke University Hospital, Stoke
Manufacturer	Siemens
Model	Revelation
System Serial Number	1679
Anode target material	Tungsten (W)
Additional filtration	50 µm Rhodium (Rh), 1 mm Titanium (Ti)
Detector type	Amorphous selenium
Detector size	304.64mm x 239.36mm
Pixel pitch	85 µm
Detector serial number	LV2-31263
Software version	VC10E and VC20*

*All images were acquired on a system running VC10 software but were later reprocessed by Siemens under the VC20 software. It is understood that the VC20 software includes updates to the TiCEM post processing and that the VC10 software is being phased out. According to Siemens there is no alteration in dose between the two versions.

2.2 Phantoms

CEM phantom

A phantom designed by Leithner et al[4] was used in the evaluation. The phantom consists of a 300 x 240 x 20 mm^3 PMMA block. Embedded within the phantom are 5 mm diameter discs containing Iopamidol at concentrations ranging from 0.25 to 2 mg cm^{-2} of iodine. Discs containing 0 mg cm^2 iodine are also included in the phantom, as well as air-filled discs. Figure 1 shows an example subtracted image of the central region of the phantom whilst Figure 2 shows the composition of each disc within the matrix of 8 columns and 5 rows.

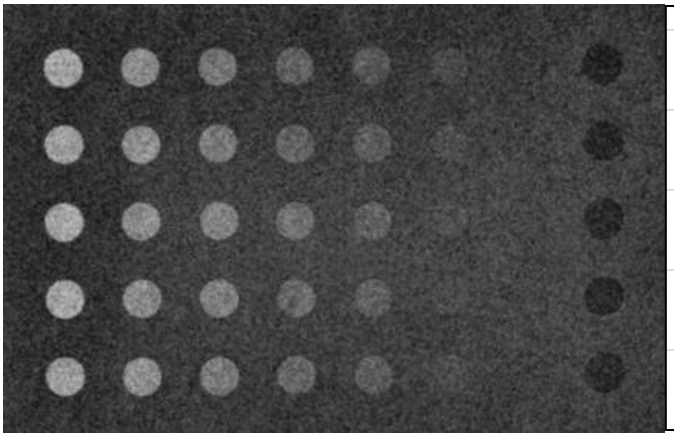

2	1.5	1	0.75	0.5	0.25	0	Air
2	1.5	1	0.75	0.5	0.25	0	Air
2	1.5	1	0.75	0.5	0.25	0	Air
2	1.5	1	0.75	0.5	0.25	0	Air
2	1.5	1	0.75	0.5	0.25	0	Air

Figure 1. Central region of subtracted image of CEM phantom

Figure 2. Iodine concentration of each disc in CEM phantom in terms of mg cm^{-2}. Discs in final column comprised of air.

Tissue equivalent blocks

The majority of the tests were undertaken using tissue equivalent blocks produced by CIRS (Norfolk, VA, USA). These blocks are designed to have similar attenuation properties as for specific fibroglandular densities of breast tissue. Dance et al[5] described a model to be used in breast dosimetry for a range of thicknesses from 20 to 110 mm. The model includes two 5 mm thick layers of fat at the upper and lower surface of the breast as well as an expected glandularity for the central portion of the breast. CIRS blocks of different densities by mass were selected to match as closely as possible those densities, in addition to the use of 5 mm of CIRS fat blocks at the bottom and top of the stack. Tables 2 and 3 show the combinations of blocks used to simulate the different breast thicknesses with and without the CEM phantom. Overall, a good match in density was found between the required glandularities and the actual values.

Table 2. CIRS tissue equivalent material used for different phantom thicknesses in addition to two 5 mm thick fat blocks

Total phantom thickness (mm)	Target glandularity of central area (%)	Glandularity of central portion (%)	CIRS Phantom [percentage glandularity] thickness (mm)				
			Fat [0%]	30:70 [30%]	50:50 [50%]	70:30 [70%]	Glandular [100%]
20	100	100					10
30	72	70				20	
40	50	50			30		
50	33	33	10	20		10	
60	21	21	30	10		10	
70	12	12	50			10	
80	7	7	60		10		
90	4	4	70	10			

Table 3. CIRS tissue equivalent material used for different phantom thicknesses in addition to CEM phantom

Total phantom thickness (mm)	Target glandularity of central area (%)	Glandularity of central portion (%)	CIRS Phantom [percentage glandularity] thickness (mm)				
			Fat [0%]	30:70 [30%]	50:50 [50%]	70:30 [70%]	Glandular [100%]
30	72	76%			10		
40	50	52%	10		10		
50	33	34%	20	10			
60	21	22%	40				
70	12	18%	50				

2.3 X-ray tube output and half value layer

The X-ray tube output and half-value-layer (HVL) were measured as described in the IPEM protocol[6] at intervals of 3 kV or, if only a limited number of options are used clinically, then only those options were measured.

2.4 Uniformity and artefacts

Percentage non-uniformity was measured using unprocessed low energy images of the 40 mm thick PMMA block provided by Siemens for the flat field calibration of this system and following the methodology described in NHSBSP guidance.[7] Artefact evaluation was performed on low energy images. Images were viewed using a narrow window to examine any artefacts that may adversely affect clinical image quality.

2.5 Automatic exposure control repeatability

The CEM phantom was imaged with 30 mm thick breast equivalent tissue blocks (Table 3) to achieve a total thickness of 50 mm. The phantom was imaged under automatic exposure control (AEC). This was repeated until four sets of images were acquired.

Subtracted images were analysed to calculate the Signal Difference (SD) and contrast-to-noise ratio (CNR) for the 1mg/cm² iodine concentration. SD was calculated as the difference in pixel value between the iodine disc and the background region. The contrast-to-noise ratio (CNR) for each disc was calculated by dividing the SD by the root mean square of the standard deviation in the iodine disc and background region.

2.6 Variation in AEC performance and image quality with phantom thickness

The CEM phantom was imaged under AEC with varying combinations of tissue equivalent blocks, as shown in Table 3. According to Siemens, the TiCEM post-processing relies on segmentation masks calculated from the low energy images. This segmentation is optimised for breast images

and so segmentation errors may occur for images of thin phantoms covering the full detector. In order to avoid these problems, for this part of the test, the segmentation mask for the 40mm phantom in table 3 was applied by Siemens for the 30mm phantom and the sole CEM phantom. Images were analysed to determine the SD and CNR for each iodine concentration. The SDs and CNRs quoted in this report are the mean values for the five identical discs of each iodine concentration. Error bars on plots indicate twice the standard error in the mean as determined from the five duplicates.

2.7 Mean glandular dose

Exposures were carried out under AEC using the combinations of tissue equivalent blocks specified in Table 2. The exposure factors were noted and mean glandular doses (MGDs) were calculated for equivalent breast thicknesses using standard methods by Dance et al.[5,8]

The MGD indicated by the system was taken from the DICOM header for both exposures and compared with the calculated value.

2.8 Subtraction of breast tissue like structure

Small samples of iodine contained in a phantom were imaged with simulated breast tissue (Leeds test objects TORMAM phantom) to assess whether the system could successfully subtract the tissue-like structures to reveal the iodine samples.

3. Results

3.1 X-ray tube output and half value layer

The X-ray tube output and HVL measurements for the system in high energy mode are shown in Table 4. Measurements were performed with the compression paddle in the X-ray beam.

Table 4. X-ray tube standard output and HVL measurements for high energy CEM image exposure parameters

kV, Target/Filter	Tube Output (µGy/mAs @ 100 cm)	HVL (mm aluminium)
45 kV W/Ti	1.86	2.84
47 kV W/Ti	2.27	3.09
49 kV W/Ti	2.73	3.31

3.2 Uniformity and artefacts

The uniformity measurement was undertaken using the 40 mm thick PMMA block, provided by Siemens for the flat field calibration of the system, positioned at the tube head. Percentage non-uniformity was measured using unprocessed low energy images. The maximum variation in pixel value from the centre of the image was 0.7%. This is well below the NHSBSP remedial level of 10%.

Artefact evaluation was performed on low energy unprocessed images and minimal ghosting was evident.

3.3 Automatic exposure control repeatability

Results for mAs, SD and CNR repeatability using OPDOSE AEC mode are shown in Table 5. The mAs repeatability was within the NHSBSP recommended remedial tolerance of 5%.

Table 5. Repeatability of mAs, SD and CNR for CEM exposures for 1.0 mg cm^{-2}

Max % variation from mean mAs	Low energy CEM exposure	0.3%
	High energy CEM exposure	0.1%
Max % variation from mean SD		1.7%
Max % variation from mean CNR		3.5%

3.4 Variation in AEC performance and image quality with phantom thickness

The SD and CNR results for 1.0 mg cm^{-2} iodine for images acquired using OPDOSE AEC mode are shown in Table 6, with results for other concentrations shown in Figures 3 and 4. For all iodine concentrations, when imaged in AEC mode, the SD is fairly constant with phantom thickness but falls slightly at the very highest thicknesses and the highest iodine concentration (Figure 3). The CNR is essentially constant with increasing phantom thickness, CNRs are within ± 10% of the mean across the range of phantom thicknesses for 1.0 mg cm^{-2} iodine. For the lowest and highest concentrations of iodine the CNR falls with increasing phantom thickness. The SD and CNR increase linearly with iodine concentration for any given phantom thickness (Figures 5 and 6).

Table 6. Variation in exposure parameters, SD and CNR for CEM subtracted images acquired in OPDOSE AEC mode for 1.0 mg cm^{-2}

Phantom thickness (mm)	kV Target/Filter		SD	CNR
	Low energy exposure	High energy exposure		
20	26 kV W/Rh	49 kV W/Ti	254.1	3.3
30	27 kV W/Rh	49 kV W/Ti	259.1	3.2
40	28 kV W/Rh	49 kV W/Ti	255.1	3.1
50	29 kV W/Rh	49 kV W/Ti	242.6	3.0
60	30 kV W/Rh	49 kV W/Ti	223.8	3.0
70	31 kV W/Rh	49 kV W/Ti	209.5	2.9

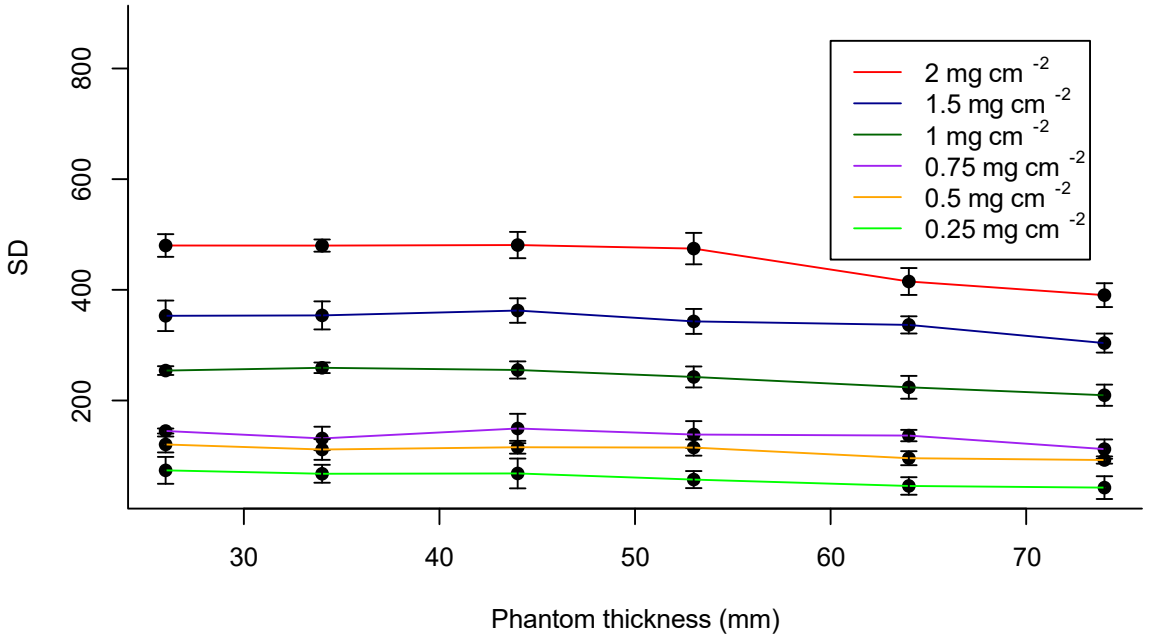

Figure 3. SD with varying phantom thickness for different concentrations of iodine (mg cm^{-2})

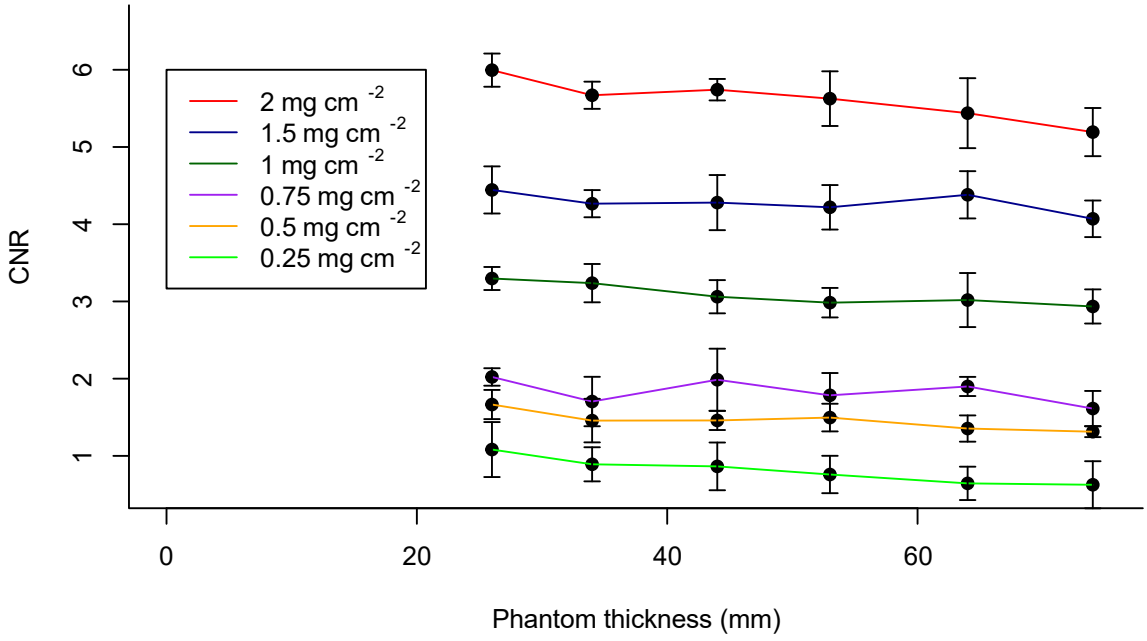

Figure 4. CNR with varying phantom thickness for different concentrations of iodine (mg cm^{-2})

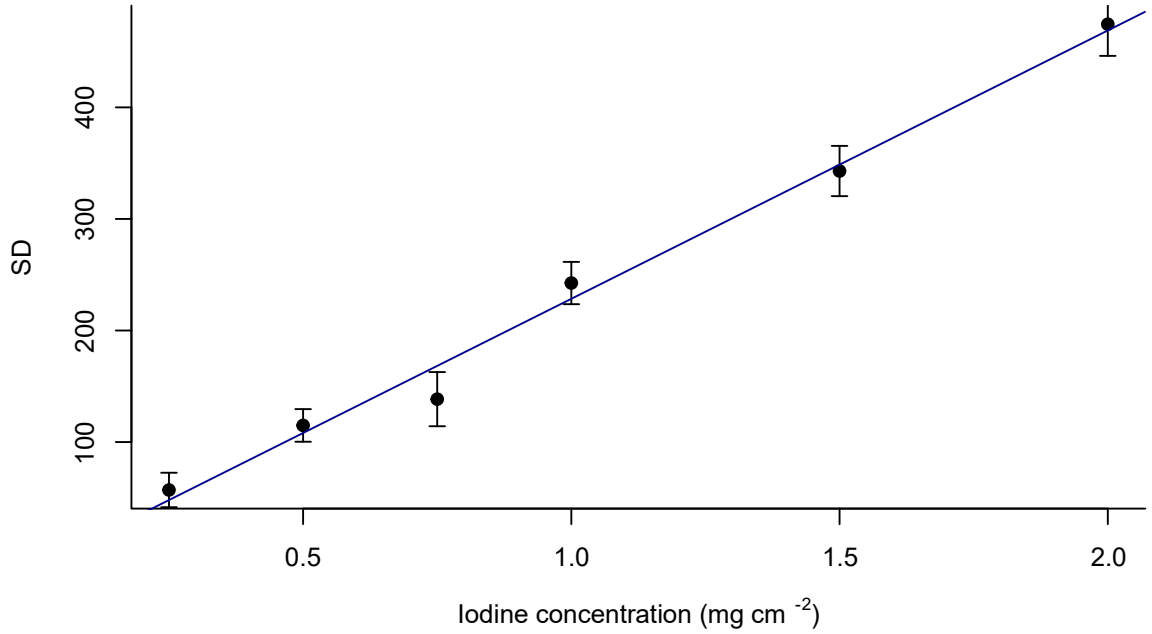

Figure 5. SD with varying iodine concentration for 50 mm thick phantom

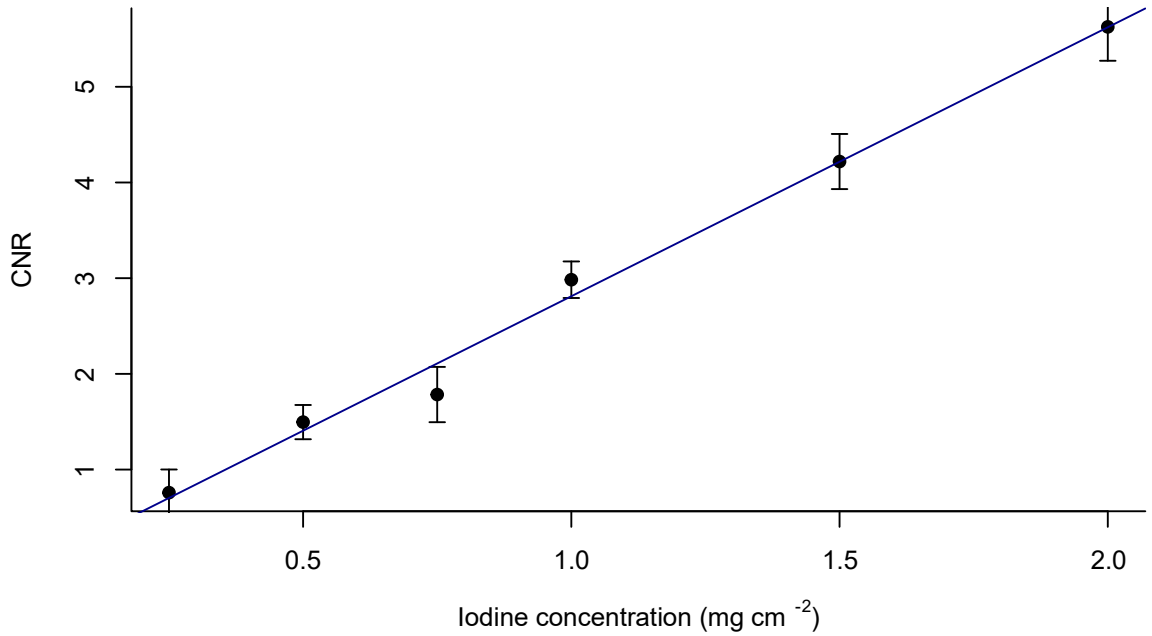

Figure 6. CNR with varying iodine concentration for 50 mm phantom thickness

3.5 Mean glandular dose

The MGDs for the tissue equivalent blocks with and without the CEM phantom acquired under OPDOSE AEC are shown in tables 7 and 8 respectively. MGDs for PMMA blocks are shown in table 9. The value of *s* used in the calculation of MGD for the W/Ti target filter combination was 1.0.

Table 7. MGDs for exposures carried out using CEM phantom with additional tissue equivalent material

Phantom thickness (mm)	Glandularity (%)	Exposure parameters (kV Target/Filter)		Calculated MGD (mGy)		
		Low energy exposure	High energy exposure	Low energy exposure	High energy exposure	Total
20	97	26 W/Rh, 35.3 mAs	49 W/Ti, 17.8 mAs	0.38	0.26	0.64
30	76	27 W/Rh, 48.1 mAs	49 W/Ti, 20.8 mAs	0.52	0.30	0.82
40	52	28 W/Rh, 64.0 mAs	49 W/Ti, 24.5 mAs	0.70	0.34	1.04
50	34	29 W/Rh, 80.2 mAs	49 W/Ti, 28.7 mAs	0.89	0.39	1.28
60	22	30 W/Rh, 98.8 mAs	49 W/Ti, 33.7 mAs	1.11	0.44	1.55
70	18	31 W/Rh, 129.5 mAs	49 W/Ti, 40.3 mAs	1.49	0.51	2.00

Table 8. MGDs for exposures carried out using tissue equivalent material only

Phantom thickness (mm)	Glandularity (%)	Exposure parameters (kV Target/Filter)		Calculated MGD (mGy)		
		Low energy exposure	High energy exposure	Low energy exposure	High energy exposure	Total
20	100	25 W/Rh, 37.3 mAs	49 W/Ti, 16.8 mAs	0.47	0.26	0.73
30	70	26 W/Rh, 52.9 mAs	49 W/Ti, 20.1 mAs	0.58	0.30	0.88
40	50	27 W/Rh, 62.7 mAs	49 W/Ti, 23.1 mAs	0.67	0.33	1.00
60	21	29 W/Rh, 107.2 mAs	49 W/Ti, 32.7 mAs	1.19	0.45	1.64
70	12	30 W/Rh, 130.6 mAs	49 W/Ti, 40.0 mAs	1.49	0.53	2.02
80	7	31 W/Rh, 165.2 mAs	49 W/Ti, 46.2 mAs	1.93	0.59	2.52
90	4	32 W/Rh, 186.6 mAs	49 W/Ti, 55.0 mAs	2.18	0.68	2.86

Table 9. MGDs for exposures carried out using PMMA

Phantom thickness (mm)	Equivalent breast thickness (mm)	Exposure parameters (kV Target/Filter)		Calculated MGD (mGy)		
		Low energy exposure	High energy exposure	Low energy exposure	High energy exposure	Total
20	21	26 W/Rh, 36.8 mAs	49 W/Ti, 18.4 mAs	0.45	0.28	0.73
30	32	27 W/Rh, 55.0 mAs	49 W/Ti, 22.5 mAs	0.61	0.32	0.93
40	45	28 W/Rh, 82.9 mAs	49 W/Ti, 27.7 mAs	0.89	0.38	1.28
45	53	29 W/Rh, 94.4 mAs	49 W/Ti, 30.9 mAs	1.03	0.41	1.44
50	60	30 W/Rh, 107.2 mAs	49 W/Ti, 34.6 mAs	1.22	0.45	1.66
60	75	31 W/Rh, 151.9 mAs	49 W/Ti, 42.1 mAs	1.67	0.51	2.18
70	90	32 W/Rh, 200.2 mAs	49 W/Ti, 53.1 mAs	2.10	0.59	2.70
80	103	32 W/Rh, 321.7 mAs	49 W/Ti, 69.1 mAs	3.04	0.73	3.77

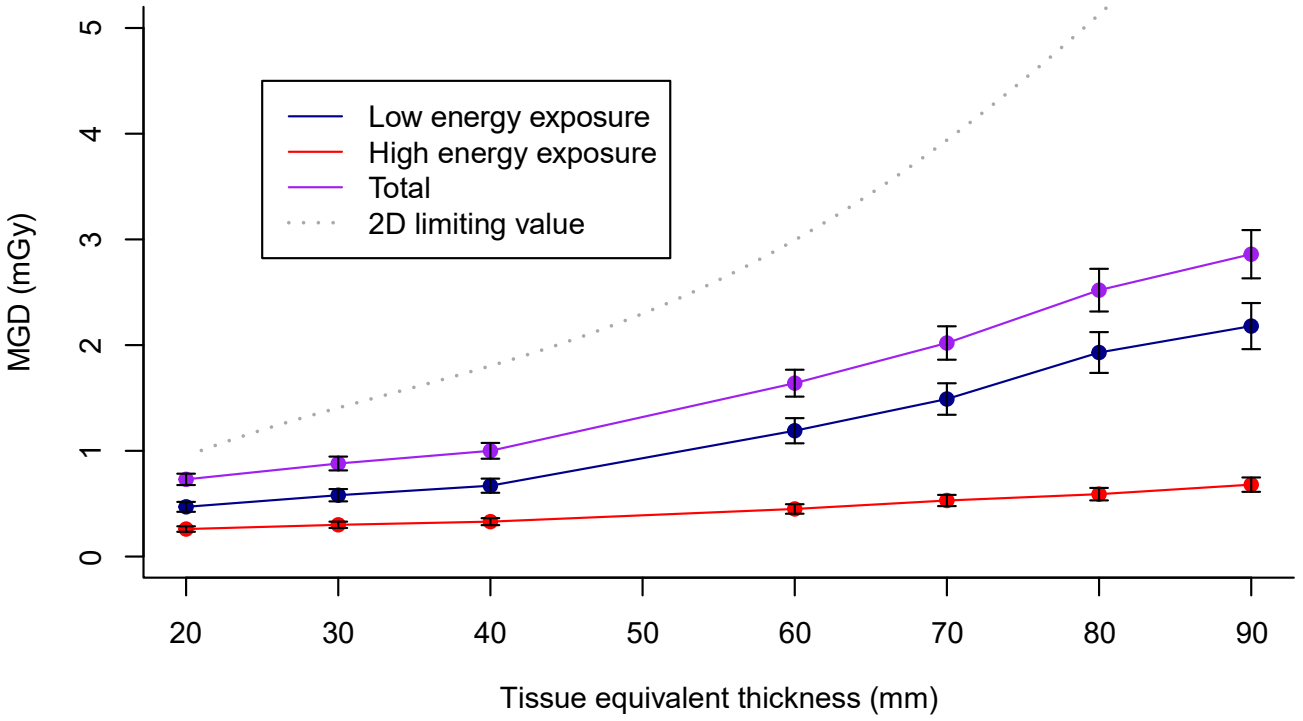

Figure 7. MGD for tissue equivalent material

The MGDs for tissue equivalent material are shown in Figure 7CEM is a different imaging modality from standard 2D imaging and so the limiting dose values are not applicable, but it is of interest to

compare them. It can be seen that the calculated total MGD is well below the limiting dose value for 2D screening for all thicknesses.

3.6 Accuracy of Indicated MGD

Table 10. Accuracy of indicated MGD

Phantom thickness (mm)	MGD (mGy) for low energy exposure			MGD (mGy) for high energy exposure			Difference for total MGD
	Calculated	Indicated	Difference	Calculated	Indicated	Difference	
20	0.47	0.55	15.0%	0.26	0.29	9.5%	15.1%
30	0.58	0.70	17.2%	0.30	0.34	13.2%	18.9%
40	0.67	0.75	10.6%	0.33	0.39	14.4%	13.5%
60	1.19	1.15	-3.0%	0.45	0.52	13.9%	2.3%
70	1.49	1.34	-11.1%	0.53	0.61	13.4%	-3.3%
80	1.93	1.67	-15.7%	0.59	0.68	13.2%	-6.8%
90	2.18	1.84	-18.6%	0.68	0.78	13.2%	-8.4%

Table 10 shows the difference between the calculated MGD and the MGD shown by the system for tissue equivalent material only. The maximum difference between the indicated and calculated MGDs was -18.6% for the low energy exposure, 14.4% for the high energy exposure and 18.9% for the total MGD.

3.7 Subtraction of BR3D Tissue-Equivalent Material

Figures 8 and 9 demonstrate the subtraction of the tissue-like structures in the TORMAM phantom to reveal the iodine samples. Some residual signal from the background structure remains in the subtracted image.

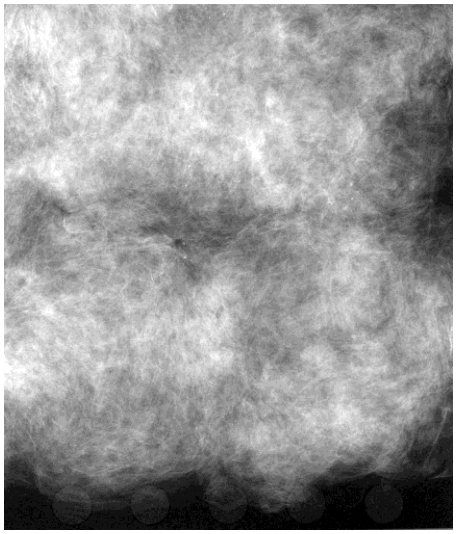

Figure 8. Low energy image of iodine samples with TORMAM

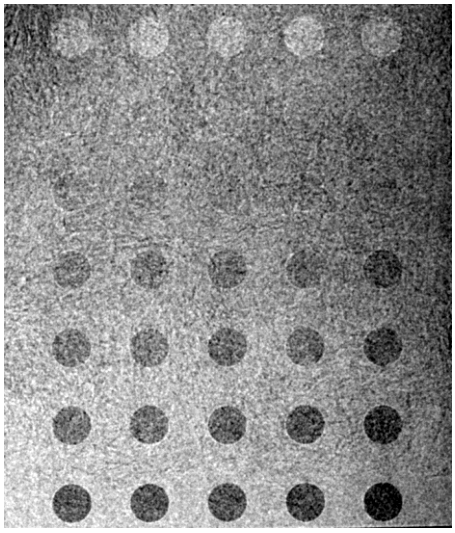

Figure9. Subtracted image of iodine samples with TORMAM

4. Discussion

4.1 Detector uniformity

- Percentage non-uniformity measured using an unprocessed images of PMMA was 0.7%. Only minor artefacts, which are not expected to be seen on clinical images, were observed

4.2 Automatic exposure control

- Exposures in OPDOSE AEC mode were repeatable in terms of mAs, SD and CNR.

4.3 Mean glandular dose

- The total MGD for a CEM exposure is between 1.3 and 1.6 times the MGD of the low energy exposure alone for phantom thicknesses ranging from 20 mm to 90 mm. The total MGDs are well below the dose limiting values for 2D screening mammography.
- The maximum deviation between the indicated and calculated MGD was -18.6% for the low energy CEM exposure and 14.4% for the high energy CEM exposure, with a maximum error of 18.9% for the total MGD.

4.4 Image quality

- For all iodine concentrations, when imaged in OPDOSE AEC mode, the SD is fairly constant with increasing phantom thickness dropping slightly for the very thickest phantoms. The CNR is reasonably constant with increasing phantom thickness, and is within ± 10% of the mean across the range of phantom thicknesses for 1.0 mg cm^{-2} iodine. The SD and CNR increase linearly with iodine concentration for any given phantom thickness.

4.5 Image subtraction

- The system was able to subtract some tissue-like structures to reveal iodine samples imaged. Some residual signal from the background structure remains in the subtracted image. According to the manufacturer, the amount of structural background noise can be adjusted in relationship to the sharpness enhancement of the lesions.

5. Conclusions

The system was able to successfully produce subtracted images with CNRs that varied linearly with iodine concentration and that were broadly insensitive to phantom thickness. As with all systems the clinical images should be audited by clinical staff.

References:

1. Oduko, J., Homolka, P., Jones, V. and Whitwam, D. A Protocol for Quality Control Testing for Contrast-Enhanced Dual Energy Mammography Systems. In: Fujita H., Hara T. and Muramatsu C. eds. *IWDM 2014: Breast Imaging, 29 June – 2 July 2014,* Gifu City, Japan. Switzerland: Lecture Notes in Computer Science, Springer, Cham. 8539, pp. 407-414.

2. Oduko, J., Homolka, P., Jones, V. and Whitwam, D. Dose and Image Quality Measurements for Contrast-Enhanced Dual Energy Mammography Systems. Proceedings of SPIE, Medical Imaging 2015: Physics of Medical Imaging. Proceedings of SPIE. 2015, 9412, 94125I-1.

3. Tyler N, Mackenzie A. Technical evaluation of Siemens Revelation digital mammography system in 2D mode (NHSBSP Equipment Report). London: Public Health England, 2019.

4. Leithner R, Knogler T, Homolka P. Development and production of a prototype iodine contrast phantom for CEDEM, Physics in Medicine and Biology, 2013, 58, N25-35.

5. Dance, D.R., Skinner, C.L., Young, K.C., Beckett, J.R. and Kotre, C.J. Additional factors for the estimation of mean glandular breast dose using the UK mammography dosimetry protocol. Physics in Medicine and Biology. 2000, 45, pp. 3225–3240.

6. Moore AC, Dance DR, Evans DS et al. The Commissioning and Routine Testing of Mammographic X-ray Systems. York: Institute of Physics and Engineering in Medicine, Report 89, 2005.

7 Kulama E, Burch A, Castellano I et al. *Commissioning and routine testing of full field digital mammography systems* (NHSBSP Equipment Report 0604, Version 3). Sheffield: NHS Cancer Screening Programmes, 2009.

8. Dance, D.R. and Young, K.C. Estimation of mean glandular dose for contrast enhanced mammography: factors for use with the UK, European and IAEA breast dosimetry protocols. Physics in Medicine and Biology. 2014, 59, pp. 2127–2137.